Remote Sens. **2015**, *7*, 3878-3906; doi:10.3390/rs70403878

OPEN ACCESS

remote sensing

ISSN 2072-4292

www.mdpi.com/journal/remotesensing

Article

Comparing MODIS Net Primary Production Estimates with Terrestrial National Forest Inventory Data in Austria

Mathias Neumann [1,*], Maosheng Zhao [2], Georg Kindermann [3] and Hubert Hasenauer [1]

[1] Institute of Silviculture, Department of Forest and Soil Sciences, University of Natural Resources and Life Sciences, Vienna, Peter-Jordan-Str. 82, A-1190 Vienna, Austria; E-Mail: hubert.hasenauer@boku.ac.at

[2] Department of Geographical Sciences, University of Maryland, College Park, MD 20742, USA; E-Mail: zhaoms@umd.edu

[3] Natural Hazards and Landscape, Department of Forest Growth and Silviculture, Federal Research and Training Centre for Forests, Vienna, Seckendorff-Gudent-Weg 8, A-1130 Vienna, Austria; E-Mail: georg.kindermann@bfw.gv.at

* Author to whom correspondence should be addressed; E-Mail: mathias.neumann@boku.ac.at; Tel.: +43-1-47654-4078; Fax: +43-1-47654-4092.

Academic Editors: Randolph H. Wynne and Prasad S. Thenkabail

Received: 11 December 2014 / Accepted: 17 March 2015 / Published: 1 April 2015

Abstract: The mission of this study is to compare Net Primary Productivity (NPP) estimates using (i) forest inventory data and (ii) spatio-temporally continuous MODIS (MODerate resolution Imaging Spectroradiometer) remote sensing data for Austria. While forest inventories assess the change in forest growth based on repeated individual tree measurements (DBH, height *etc.*), the MODIS NPP estimates are based on ecophysiological processes such as photosynthesis, respiration and carbon allocation. We obtained repeated national forest inventory data from Austria, calculated a "ground-based" NPP estimate and compared the results with "space-based" MODIS NPP estimates using different daily climate data. The MODIS NPP estimates using local Austrian climate data exhibited better compliance with the forest inventory driven NPP estimates than the MODIS NPP predictions using global climate data sets. Stand density plays a key role in addressing the differences between MODIS driven NPP estimates *versus* terrestrial driven inventory NPP estimates. After addressing stand density, both results are comparable across different scales. As forest management changes stand density, these findings suggest that management issues are important in understanding the observed discrepancies between MODIS and terrestrial NPP.

Keywords: forest; NPP; management; inventory; MODIS; Austria

1. Introduction

Productivity estimates are important measures to characterize the mass budget of a forest ecosystem. In this context, the carbon balance and carbon storage of the earth's ecosystems and their spatial and temporal development is important. A measure for the carbon flux is Net Primary Production (NPP) which describes the carbon uptake by vegetation through photosynthesis. In principle, large scale carbon measures are currently provided by National Forest Inventories, flux towers and remotely sensed methods, such as the MODIS (MODerate resolution Imaging Spectroradiometer) NPP algorithm.

Researchers in previous studies have compared MODIS satellite-driven NPP with NPP estimates derived using terrestrial data [1–3]. Shvidenko *et al.* [1] found that for Russia the two estimates comply on average. Pan *et al.* [2] observed deviations between MODIS and terrestrial NPP using inventory data from the mid-Atlantic region of the USA and suggest that differences in water availability explain this variation. Hasenauer *et al.* [3] also found similar deviations and concluded that the different data sources for predicting NPP compare well after addressing forest management impacts. The authors further suggest that a combination of "ground-based" forest data with "space-based" forest productivity estimates would utilize the advantages of both methods.

National forest inventories are established for a continuous monitoring of the forest situation across countries. They are often based on a systematic permanent grid design. For each sample plot, a limited number of trees compared to the total forest area [4] is recorded to provide information on the standing growing stock, increment, species composition and other information needs relevant for forest management [5,6]. Such forest inventories are usually repeated every five to 10 years. Examples for national long term forest inventories can be found in countries such as Austria, Norway, Finland, Germany, *etc.* [4].

The MODIS NPP algorithm is based on remote sensing techniques and was developed for estimating large-scale forest productivity [7,8]. MODIS is a satellite-mounted sensor operated by the National Aeronautics and Space Administration of the United States (NASA) that provides large-scale information on global dynamics and processes. The MODIS algorithm MOD17 uses satellite data, climate data and biophysical properties of various cover types to derive eight-day GPP (Gross Primary Production) and NPP estimates on a 1 × 1 km pixel resolution. This data source may be seen as a "space-based" approach and provides continuous coverage across the global land area to assess forest productivity.

The differences of the two approaches are as follows:

(i) The MODIS satellite-driven NPP is based on the principles of carbon uptake following light use efficiency logic [9] using a simplification of the NPP algorithms implemented in BIOME-BGC [10]. According to the hypothesis put forth by Hasenauer *et al.* [3] the MODIS NPP algorithm assumes a fully stocked forest for a given vegetation class or biome type and provides eight-day results NPP estimates on a 1 × 1 km grid.

(ii) NPP estimates derived from terrestrial forest growth data (permanent sampling plots or forest inventory data) employ biomass expansion factors or biomass functions based on repeated observations such as breast height diameter (*dbh*) and/or tree height (*h*). Depending on the measurement interval the derived increment results represent a mean periodic average. Since this method is based on individual tree observations (e.g., *dbh*, *h*), potential changes in tree growth due to stand age, stand density or environmental effects such as weather patterns or CO_2 concentration are included as they affect *dbh* and *h* development.

Several studies have compared satellite to terrestrial inventory data [1,2,11–16], however, no analysis has compared forest inventory data to MODIS NPP in Central Europe.

The mission of this paper is to compare space-based MODIS satellite-driven NPP data to ground-based inventory data driven NPP estimates using the Austrian National Forest Inventory Data. This Forest Inventory is based on a systematic permanent grid design with repeated observations [5,17]. The objectives of our study are:

(i) obtain MODIS NPP estimates (using different climate data) for comparing the results with terrestrial-driven NPP estimates

(ii) examine the potential effects of stand density, MODIS land cover types, stand age, species composition, ecoregion and elevation on NPP estimates by method.

2. Methods

2.1. MODIS NPP—"Space Based" Approach

We use the algorithms for the MODIS products MOD17A2 and MOD17A3, which provide global Gross and Net Primary Production (GPP, NPP) estimates for a 1 × 1 km pixel on an eight-day time-step [7,8]. The algorithm calculates *GPP* as

$$GPP = LUE_{\max} \times 0.45 \times SWrad \times FPAR \times f_{VPD} \times f_{Tmin} \quad (1)$$

where LUE_{max} is the maximum light use efficiency, *SWrad* is the short wave solar radiation load at the surface of which 45% is photosynthetically active, *FPAR* the fraction of absorbed PAR (Photosynthetic Active Radiation) from the MOD15 product, and f_{VPD} and f_{Tmin}, which are multipliers between 0 and 1 addressing water stress due to vapor pressure deficit (*VPD*) and low temperature limits (T_{min}, daily minimum temperature). Values that determine the LUE_{max} and the T_{min} and *VPD* multipliers limits are stored in the Biome Property Type Look Up Tables (BPLUT) and cover five forest biome types: (i) ENF—Evergreen Needleleaf Forest, EBF—Evergreen Broadleaf Forest, DNF—Deciduous Needleleaf forest, DBF—Deciduous Broadleaf Forest, and MF—Mixed Forests ([3] for the model coefficients).

Annual Net Primary Production (*NPP*) is calculated from Gross Primary Production (*GPP)* by subtracting the autotrophic respiration components (i) maintenance respiration R_m and (ii) growth respiration R_g and summing up over a year to get annual values:

$$NPP = \sum_{i=1}^{365} GPP - R_m - R_g \quad (2)$$

With 366 days for leap years, R_m and R_g are calculated using leaf area index (*LAI*) from the MOD15 product, climate data, and parameters from the BPLUTs. For further details, please refer to the original literature [7,8].

2.2. Terrestrial NPP—"Ground Based" Approach

NPP can be calculated as the sum of biomass increment, mortality, and turnover of foliage and fine roots [18]. We employ volume and biomass functions along with repeated observations to get increment and mortality. Turnover of foliage, including mortality of other plant components, is represented by a climate-sensitive litterfall model [19]. The advantage of this model is the requirement of little input data and assumptions compared to calculating litterfall using biomass and turnover rates [18]. We lack a reliable model for fine root turnover in Austria and we assume that carbon uptake of fine roots is already incorporated in litterfall and coarse root increment.

2.2.1. Increment Estimation

Originally forest growth data was intended to provide volume increment in m^3/ha per growth period [6]. The growth period varies depending on the temporal measurement interval of terrestrial sample plots. We develop a consistent and comparable terrestrial productivity data set by deriving NPP estimates using forest inventory data starting with:

$$NPP = inc_{plot} + C_{Litter} \tag{3}$$

where C_{Litter} is the flow of dry carbon into litter [gC/m^2/year] as defined in Equation (9), inc_{plot} is the dry carbon increment of trees (above and below ground biomass) [gC/m^2/year] resulting from repeated plot observations taken at the end C_{Forest_2} minus those observations taken at the beginning C_{Forest_1} of the growth period

$$inc_{plot} = C_{Forest\_2} - C_{Forest\_1} \tag{4}$$

Equation (4) gives the common way to calculate increment for repeated observations and terrestrial plot data, the carbon values (C_{Forest_1} and C_{Forest_2}) being the sum of the tree carbon estimates calculated from repeatedly measured diameters at breast height (*dbh*) and tree heights (*h*) for a given tree. The National Forest Inventory of Austria use a combined recording system with (i) fixed area plots for trees ranging in *dbh* from 5 cm to 10.4 cm and (ii) an angle count sampling system [20] for all trees with a *dbh*>10.4 cm. In angle count sampling the stem number represented by a sample tree changes by diameter and thus the represented tree population changes too, which differs from fixed-area plots (e.g., used in the National Forest Inventory system of Norway [4] or permanent research plots like the "Austrian Waldboden-Zustandsinventur" [21]). This affects volume or biomass stocks as well as periodic increment and thus the results from fixed area plot sampling are quite different compared to angle count sampling [6].

In principle, three different approaches in estimating increment form angle count sample data exist: (i) the starting value method; (ii) the end value method and (iii) the difference method.

For details we refer to Schieler [22] and Hasenauer and Eastaugh [6]. All three methods are statistically sound and deliver unbiased results [23,24].

For our study, we use the starting value method, which is also used by the Austrian National Forest Inventory:

$$inc_{plot} = \Sigma inc_{survivors} + \Sigma inc_{ingrowth} \quad (5)$$

where inc_{plot} is the periodic increment on each plot resulting from $\sum inc_{survivors}$ the "survivor trees", which were also sampled in the last measurement, and $\sum inc_{ingrowth}$ the "ingrowth trees" or trees, which have reached the threshold during the re-measurement period and are thus selected [6,22,25]. The carbon increments of the "survivor trees" are calculated as

$$\Sigma inc_{survivors} = \Sigma((C_2 - C_1) \times nrep_1) \quad (6)$$

and the carbon increments of the "ingrowth trees" are

$$\Sigma inc_{ingrowth} = \Sigma(C_2 \times nrep_2) \quad (7)$$

$nrep_i$ is the "represented" stem number per hectare at time 1 or time 2 and depends on the basal area factor k and the individual tree basal area g (for trees with dbh >10.4 cm $nrep_i = k/g$ and for trees with dbh 5–10.4 cm $nrep_i$ = 10,000/(2.6$^2\pi$) = 470.9). C_i are the carbon estimates for this "representative" tree at time 1 or time 2.

2.2.2. Carbon Estimation

The carbon increment calculation requires carbon estimates for each tree on a given inventory plot. For our study, we use the same method as applied by the Institute of Forest Inventory, Federal Research Centre for Forest, the agency responsible for the National Forest Inventory in Austria. The total dry carbon tree estimates of a single tree, C_i, can be calculated as follows:

$$C_i = CC \times (dsm + dbm + dfm + drm) \quad (8)$$

where CC is the carbon content and considered to be 0.5 for all species [26], dsm is the dry stem mass including bark, dbm the dry branch mass, dfm the dry foliage mass and drm the dry root mass with a diameter >2 mm.

The calculation of tree biomass is done using volume and biomass functions developed and used in Austria (see Appendix).

2.2.3. Litterfall Estimation

The last compartment for estimating NPP from terrestrial data in Equation (3) is the carbon flow into litter (C_{Litter}). We select the method proposed by Liu *et al.* [19], which calculates the forest litter fall including all aboveground plant compartments according to Equations (9) and (10):

$$C_{Litter} = CC \times LF \quad (9)$$

$$\ln(LF) = 2.296 + 0.741 \times \ln(T + 10) + 0.214 \times \ln(P) \quad (10)$$

C_{Litter} is the carbon in litterfall [gC/m^2/year], CC carbon content equal 0.5 [26], LF total litter fall [g·dry·biomass/m^2/year], T the mean annual temperature 2000–2010 [°C], P mean annual precipitation 2000–2010 [mm].

2.2.4. Stand Density Calculation

Forest management reduces stand density, stand density affects individual tree growth and thus the "ground-based" terrestrial NPP predictions [3]. For characterizing the stand density variation on the inventory plots we select the following two commonly used competition measures: *CCF* the crown competition factor [27] with Equation (11) and *SDI* the stand density index [28] with Equation (14):

$$CCF = \frac{\sum PCA_i \times nrep_i}{A} \times 100\% \quad (11)$$

Where PCA_i the species-specific potential crown area [m^2] according to Equations (12) and (13)

$$PCA_i = (\frac{CW_i}{2})^2 \times \pi \quad (12)$$

$$CW_i = e^{c_0 + c_1 \times \ln(dbh)} \quad (13)$$

with $nrep_i$ as the representative stem number [ha^{-1}] and A the observed area. CW_i is the potential crown width [m] and *dbh* the diameter at breast height [cm]. The PCA_i defines the crown area of a tree assuming open-grown conditions (the tree never experienced competition). Coefficients c_0 and c_1 in Equation (13) are derived from open-grown tree dimensions [29] and are given in Table A6 in the Appendix.

The Stand Density Index (*SDI*) is calculated according to Reinecke [28]:

$$SDI = N\left(\frac{dg}{25}\right)^{1.605} \quad (14)$$

where N is the number of trees per unit area [ha^{-1}], dg is the quadratic mean stand diameter at breast height [cm], 25 is a reference dg and 1.605 is the slope parameter for the maximum carrying capacity. The SDI has been proven to be site and age independent and SDImax defines an estimate for the carrying capacity of a given forest type [30].

2.2.5. Determining the Dominant Tree Species and the Ecoregions

One important aspect of our study is to assess potential effects of tree species on the MODIS and the NFI-driven productivity estimates. A grouping of the dominant tree species is done according to the main relative proportion of the basal area at a given inventory plot. The Norway Spruce (*Picea abies* (L.) Karst) and the Silver Fir (*Abies alba* Mill.), as relatively shade-tolerant species, are combined in one group. The Scots Pine (*Pinus sylvestris* (L.) Karst.) and the European Larch (*Larix decidua* Mill.) are light-demanding pioneer species and are also combined in one group. The two main broadleaf species groups are the Common Beech (*Fagus sylvatica* (L.)) and the Oak (*Quercus spp.*). These four groups cover 89% of the inventory plots. The remaining 11% are dominated by tree species which are aggregated into two groups: other coniferous trees and other broadleaf trees.

Austria has some very distinct biogeographic growth conditions due to the east-west aligned Alps. According to Kilian *et al.* [31], these differences lead to typical ecoregions (see Figure 1) and are characterized by similar environmental, macro-climatic as well as geological conditions leading to

differences in potential vegetation. To assess the potential effect of these drivers, we assign the ecoregions to each inventory plot according to the plot location as outlined in Figure 1. With the ecoregions, we then can also examine the effect of geographical location on the results.

3. Data

3.1. Climate Data

Climate data is required as input to the MOD17 algorithms that derive MODIS NPP and for estimating the carbon content in the litterfall with Equations (9) and (10). Daily records of minimum and maximum temperature, precipitation, vapor pressure deficit and incident short wave radiation are interpolated from weather station data using DAYMET, a climate interpolation model [10] adapted and validated for Austrian conditions [32,33]. DAYMET interpolates daily precipitation and minimum and maximum temperatures from surrounding permanent climate stations. Based on the resulting climate data, daily solar radiation and vapor pressure data are calculated [34]. The current version of DAYMET [35] requires longitude, latitude, elevation, slope, aspect and the horizon angle facing east and west for each given plot. The meteorological data for running DAYMET were provided by the Austrian National Weather Center (ZAMG) in Vienna and include daily weather records from 250 stations across Austria since 1961. For our analysis, we generate daily weather data at a 1 × 1 km grid across the country.

For the MODIS NPP calculations we also use two additional climate data sets called "GMAO" and "NCEP2", which are described in the next chapter.

3.2. MODIS Data

The storage system of MODIS data consists of 286 vegetated land tiles covering the whole globe. Each tile covers an area of 1200 × 1200 km or 1.44 million pixels. The MOD17 algorithm provides an eight-day GPP/NPP estimate for each 1 × 1 km pixel. We sum eight-day values to annual. We use the MODIS NPP product developed by Zhao *et al.* [36].

Previous studies showed that the direct use of 1 × 1 km MODIS pixel for validation may be inappropriate [37–39]. Reported reasons are (i) mismatch between MODIS gridded pixels and observations caused by gridding artifacts [38]; (ii) problems in the mixed land cover and surface reflectance information and (iii) uncertainties in the information provided for building the look-up tables [38]. We follow previous studies [3,37–39] and obtain the mean MODIS NPP of a 3 × 3 pixel patch (nine 1 x 1 km pixels) for each inventory plot. Within these 9 pixels we select only forest pixels according to the MOD12Q1 product [8] and the classification system of Friedl *et al.* [40]. Pixels with any other land cover type are ignored. For each of the forest pixels, we take the mean value of the MODIS NPP estimates according to three different climate input data sets provided by:

(1) the NASA Global Modeling and Assimilation Offices (GMAO) at NASA Goddard Space Flight Center with a spatial resolution of 0.5 × 0.67° [41]. MODIS NPP derived from this data set will be referred to as "GMAO".
(2) the daily climate data set called NCEP_DOE_II with a spatial resolution of approx. 1.875 × 1.875° [42,43], referred to as "NCEP2".

(3) Austrian local daily climate data interpolated with DAYMET (see previous chapter) on 1 × 1 km (approx. 0.0083 × 0.0083°) resolution with station data provided by the Austrian National Weather Centre: "ZAMG".

The difference between the MODIS NPP driven by GMAO and NCEP2 is caused by the different global daily climatology drivers and correspondingly modified BPLUT file [44]. The first two data sets are maintained by the Numerical Terra Dynamic Simulation Group (NTSG) at the University of Montana, while the Austrian local climate data are maintained by the Institute of Silviculture at The University of Natural Resources and Life Science, Vienna (BOKU).

From 1 January 2000 to 31 December 2011 for 11 full years all three variants of MODIS NPP estimates are computed. Until February 2000, missing MODIS data is considered negligible. Although the data is available annually, we use the periodic mean annual NPP for these 11 years to have a consistent and comparable temporal scaling with the forest inventory data. The variation between annual and periodic mean MODIS NPP is small (mean standard deviation 37.1 gC/m^2/year) and shows no trend across Austria. The lack of trend and the low variation supports the use of the temporal aggregation.

Figure 1 gives the periodic mean annual MODIS driven NPP (2000–2011) estimates across the country and demonstrates the special feature of a "space-based" satellite-driven approach, providing continuous cover in productivity estimates for every km^2 across Austria.

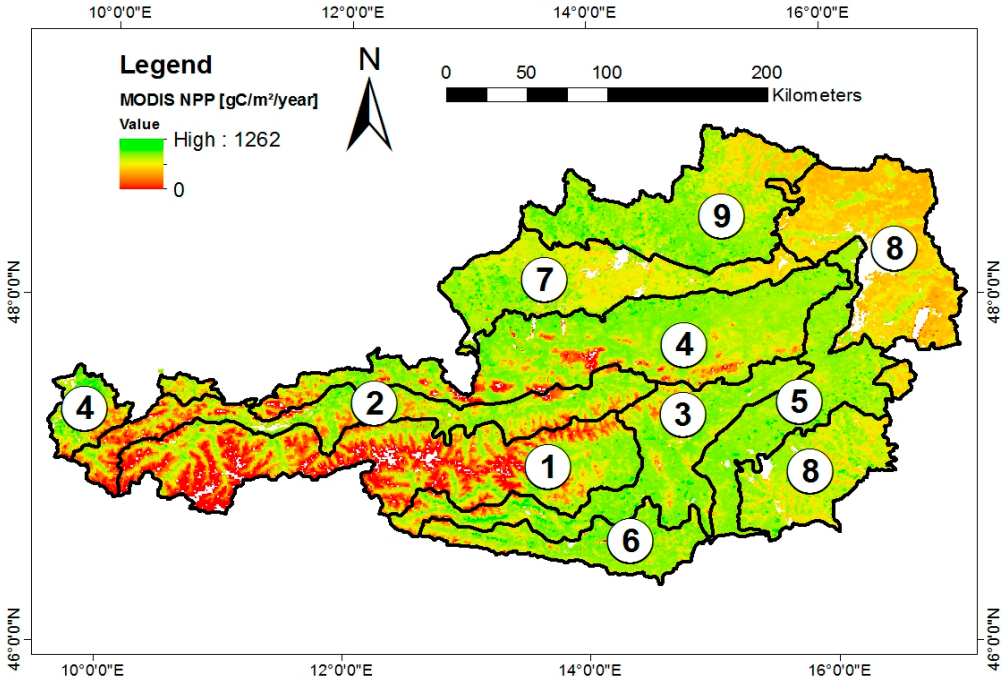

Figure 1. MODIS NPP for Austria calculated with NCEP2-climate data, black lines delineate forest ecoregions [31] used in the analysis.

3.3. Forest Inventory Data

The National Austrian Forest Inventory is based on a systematic permanent grid design of 3.889 × 3.889 km over Austria with a cluster of four inventory plots at each grid point (approx. 22,000 plots and 5500 clusters). One cluster is a square with 200 m length on each side and a plot in each

corner. The permanent plots were established during 1981–1985, where each year every 5th cluster was established. The inventory uses a hidden plot design where the center of each plot is marked with a hidden iron stick to eliminate research plot bias [45]. This is important because this procedure ensures that the Forest Inventory is representative for the growing conditions and forest management throughout Austria. The condition of the forest is measured on each plot with an angle count sample plot [20] using a basal area factor of 4 m^2/ha for trees with *dbh* ≥10.4 cm and with a fixed area plot (r = 2.6 m, A = 21.2 m^2) for trees with *dbh* ranging from 5.0 to 10.4 cm.

For details on the plot and sampling design, see Schadauer *et al.* [5] and Gabler and Schadauer [17]. For details on the applied sample methodology and its advantages and constraints, see literature [6,20,22,24,46].

We obtain the two most recent inventory measurements for our study: NFI 6, plot data recorded from 2000 to 2002, and NFI 7, plot data recorded from 2007 to 2009 resulting in a re-measurement interval of seven years [17]. We calculate periodic mean annual increment inc_{plot} with Equations (3)–(5).

Measurements of diameter at breast height (1.3 m) were taken for all sample trees. In NFI 6, tree height and height to the live crown base were only recorded for a subsample of trees on each plot. The missing estimates were estimated by applying dbh-dependent models. In NFI 7, tree height, height to the live crown base and dbh were recorded for every tree [17]. Data are available for approximately 9000 plots. Table 1 shows the summary statistics of the data available from the inventory plots for our analysis.

4. Results and Analysis

For the presented results and figures, the median is used which is less affected by outliers and skewed distributions. In the text the arithmetic mean is given, however, any comparison based on mean values assumes a symmetric distribution of the results and a balanced age class distribution of forests.

4.1. MODIS NPP versus *Terrestrial NPP*

Since three different daily climate data sets are available for deriving MODIS NPP across Austria, we explore the impact of different daily climate data on the resulting MODIS NPP computations. We compute the MOD17 NPP estimates for the years 2000–2011 using three different daily climate data sets: (i) GMAO; (ii) NCEP2 and (iii) ZAMG. For all three settings, the improved method for estimating NPP according to Zhao *et al.* [44] is used.

The mean values for the NPP results using the local climate data set (ZAMG) 568.0 gC/m^2/year (median 579.8 gC/m^2/year, standard deviation 113.6 gC/m^2/year), using the climate data of NCEP2 728.6 gC/m^2/year (median 738.9 gC/m^2/year, standard deviation 59.6 gC/m^2/year) and of GMAO 731.5 gC/m^2/year (median 742.3 gC/m^2/year, standard deviation 79.2 gC/m^2/year) (Figure 2). The NPP estimates result from the computations according to Equations (1) and (2) and the cited references. The varying NPP computation results are due to the differences in the daily climate data sets [44], as all other input parameters were kept constant.

For the same forest inventory plots we calculate the terrestrial NPP according to Equations (3)–(10) and the information given in the Appendix. Note that due to the inventory design the results cover all

trees with a *dbh* ≥5 cm. The terrestrial NPP results (NFI) are also presented in Figure 2 and show a mean of 525.2 gC/m^2/year (median 486.3 gC/m^2/year, standard deviation 251.4 gC/m^2/year). The numbers above the boxplots give the sample size. The difference between NFI and MODIS of 222 are the inventory plots, where MODIS classify a land cover other than forest. The root mean square error (RMSE) between MODIS and terrestrial NPP is for ZAMG 276.1 gC/m^2/year, for NCEP2 335.5 gC/m^2/year and for GMAO 340.3 gC/m^2/year.

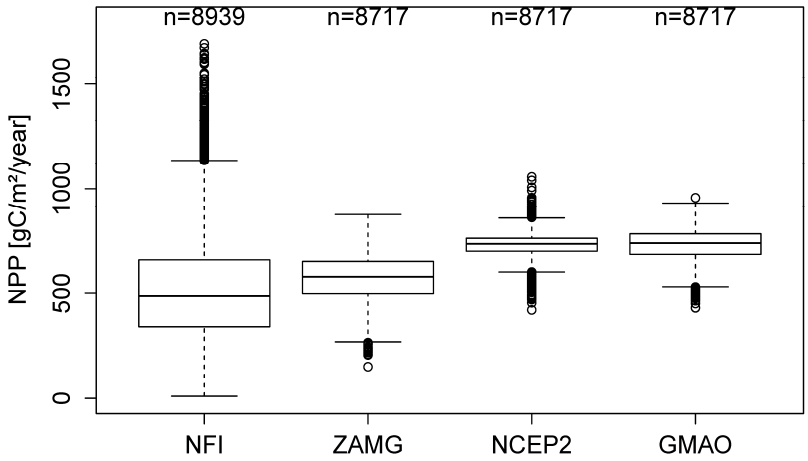

Figure 2. Comparisons of the NPP estimates where (1) *NFI*—the terrestrial NPP; (2) *ZAMG*—MODIS NPP estimates using the daily weather data from the Austrian National Weather Centre; (3) *NCEP2*—MODIS NPP estimates using the daily weather data of the so called NCEP_DOE_II [42], and (4) *GMAO*—MODIS NPP using the daily climate data from NASA Global Modeling and Assimilation Office [41]. The box represents the Median and the 25th and 75th quartile, the whiskers extend to 1.5 of the interquartile range, values outside this range are indicated by circles, and on the top the number of values represented by the boxplots is given.

4.2. Stand Density Effects

MODIS NPP estimates vary by climate input data (ZAMG, NCEP2, GMAO) and are in general higher compared to the terrestrial NPP (NFI in Figure 2). The local daily climate data set provided by the Austrian National Weather Service (ZAMG) exhibits the lowest discrepancy *versus* the terrestrial NPP estimates (RMSE 276.1 gC/m^2/year, difference of medians 93.5 gC/m^2/year, difference of means 42.8 gC/m^2/year).

Forest management reduces stand density [47–52]. Hasenauer *et al.* [3] suggested that stand density explains the observed discrepancies between "space-based" MODIS *versus* "ground-based" NPP estimates. Stand density is important considering that forest management operations change the number of trees, which directly effects the calculation of the terrestrial NPP estimates see Equations (5)–(7). In the MODIS NPP algorithm, on the other hand, forest dynamics are characterized by the two input variables FPAR and LAI, as the land cover type is kept constant. Both variables are derived from spectral properties of the vegetation, in particular the spectral signal of the red and near infrared bands [37,39]. Intensity of forest management in Austria is regulated (crown cover

after thinnings of at least 60%, while clearcuts bigger than 0.5 ha need special registration and may not exceed 2 ha) [47]. Thus, it can be assumed that forest management in Austria has only a small and temporary influence on FPAR and LAI. The results of the analysis (not shown) support this as MODIS NPP show no correlation with stand density, while terrestrial NPP clearly does, which will be shown shortly.

For assessing the potential management impacts on the results we obtain for each inventory plot two stand density measures: (i) the *CCF*—Crown Competition Factor according to Krajicek *et al.* [27] Equation (11) as well as (ii) the *SDI*—Stand Density Index according to Reinecke [28] in Equation (14). The mean and the variations across all plots are given in Table 1.

Table 1. Summary statistics of the inventory plots for period 2007–2009 by dominant tree species. Given is mean and in brackets the data range (minimum—maximum). *SDI* the Stand Density Index [28], and *CCF* the Crown Competition Factor [27].

Variable	Spruce, Fir	Larch, Pine	Other Coniferous	Beech	Oak	Other Broadleaf	All
Number of plots	5809	1001	140	886	238	864	8939
Age dominant trees	81	95	122	95	80	51	82
(a)	(15–175)	(15–175)	(15–175)	(15–175)	(15–165)	(15–175)	(15–175)
Elevation (m)	1019	914	1084	741	377	544	880
	(220–2110)	(245–2066)	(259–2212)	(244–1467)	(176–971)	(129–1685)	(129–2212)
Number of trees	1029	859	741	890	692	1141	993
(ha^{-1})	(3–10084)	(4–6205)	(5–3544)	(8–9394)	(6–5934)	(1–8917)	(1–10084)
Stem volume	361	304	268	329	220	200	331
(m^3/ha)	(2–1672)	(2–1205)	(13–726)	(2–1382)	(8–758)	(2–1281)	(2–1672)
Basal area	36	33	35	33	25	25	34
(m^2/ha)	(1–124)	(1–104)	(4–79)	(1–100)	(2–76)	(1–107)	(1–124)
SDI	738	665	679	655	512	553	697
	(36–2618)	(38–2086)	(48–1705)	(36–2066)	(49–1523)	(36–2649)	(36–2649)
CCF	204	206	188	350	209	315	229
	(7–1308)	(10–969)	(7–697)	(21–1622)	(16–625)	(11–1699)	(7–1699)

Next, we calculate the differences (ΔNPP) between the "space-based" MODIS NPP (using the Austrian daily climate data ZAMG) and the "ground-based" NPP using the NFI data set. After grouping the results by *CCF* and *SDI* classes, the median and the first and third quartile of ΔNPP *versus SDI* and *CCF* class for the total data set are plotted. A direct comparison of terrestrial inventory plots with a MODIS pixel requires the assumption that a plot is actually representative for an area, which is discussed and questioned by previous research [48,49]. However, it allows us to track the effect of stand variables, which would be otherwise impossible.

A distinct stand density related trend is visible with an overestimation of the terrestrial NPP by MODIS NPP at low stand density and an underestimation at high stand density, which is consistent whether using *SDI* or *CCF* (Figure 3).

The MODIS NPP algorithm uses information on the land cover or vegetation type provided by the classification system of the University of Maryland (MODIS Collection 5 global land cover) [8,40]. In total, there are 14 land cover classes, of which five deal with forests and characterize the biophysical properties expressed by the parameters of the Biome Property Look-Up-Tables (BPLUT) [7,8]. These

land cover types represent different tree species groups [40] and, due to different coefficients in the BPLUT, affect the MODIS NPP results [8]. Thus, next we are interested if the observed stand density related trends (Figure 3) may differ to MODIS land cover types.

Austria consists of a fragmented landscape, varying forest ownership and distinct historical management impacts. Consequently, many of our 3 × 3 km areas (nine pixels) include several forest land cover classes. To avoid any impact of this "mixture effect" we select only plots which feature nine pixels with only one MODIS land cover type. The land cover types "deciduous needleleaf forest" and "evergreen broadleaf forest" are excluded as there are very few pixel patches that have this land cover type exclusively (one for deciduous needleleaf forest, two for evergreen broadleaf forest).

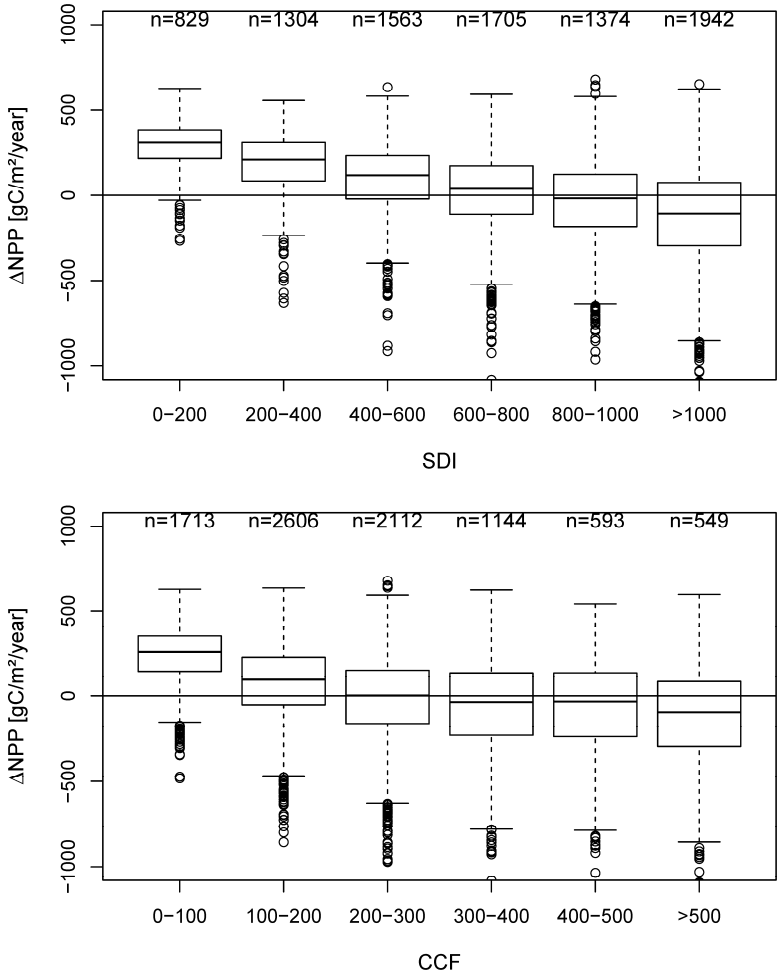

Figure 3. Difference between MODIS NPP and NFI NPP (MODIS minus NFI) grouped by stand density measures: SDI (**top**); CCF (**bottom**). Properties of illustration analogous to Figure 2.

The results for the "deciduous broadleaf forest" (not shown) are similar. To summarize, the results using plots with only one biome type exhibit the same trend when using all data (Figure 3): overestimation of terrestrial NPP by MODIS NPP at low stand density and underestimation at high stand density, which is consistent for both stand density measures (Figure 4).

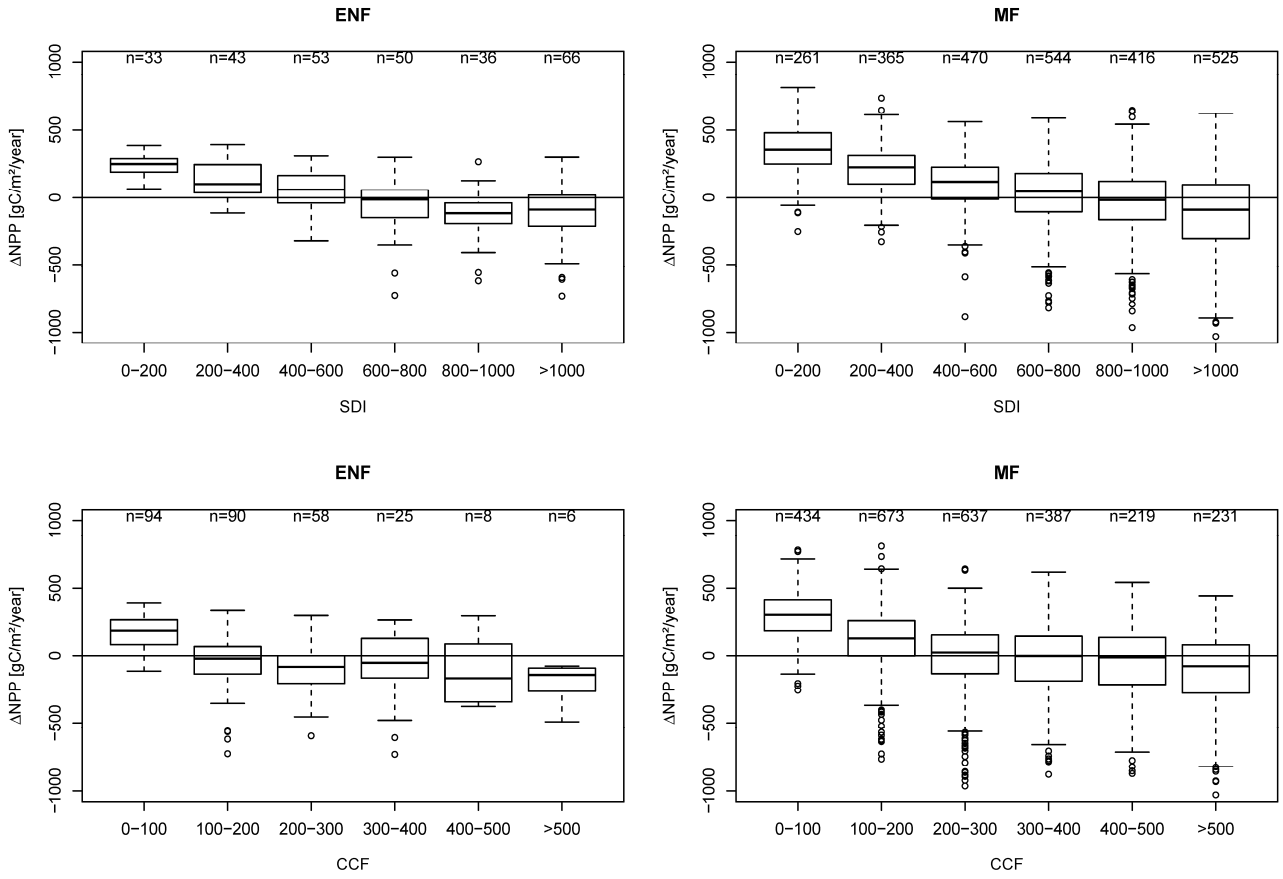

Figure 4. Difference between MODIS NPP and NFI NPP (MODIS minus NFI) grouped by MODIS land cover types (ENF = evergreen needleleaf forest, MF = mixed forest) and stand density measures: SDI (**top**); CCF (**bottom**). Properties of illustration analogous to Figure 2.

4.3. Addressing Stand Density Effects

The results in Figures 3 and 4 show a clear stand density related trend. We apply a logarithmic trend curve to correct for stand density effects similar to Hasenauer *et al.* [3]:

$$\Delta NPP = a + b \times \ln(SDI) \pm \varepsilon \quad (15)$$

$$\Delta NPP = a + b \times \ln(CCF) \pm \varepsilon \quad (16)$$

a and *b* are the corresponding coefficient estimates and ε the remaining error and all other variables as previously defined. We apply Equations (15) and (16) to all data and again separately for the three MODIS forest land cover types relevant for Austrian forests ("evergreen needleleaf forest", "mixed forest" and "deciduous broadleaf forest". Note that the stand density measures *SDI* and *CCF* are calculated based on the stand situation at the end of the growth period. Plotting the results of the fitted trend curves show that all exhibit the same pattern whether they are grouped according to *SDI* or *CCF* (left images in Figure 5). The regression results are given in Table 2.

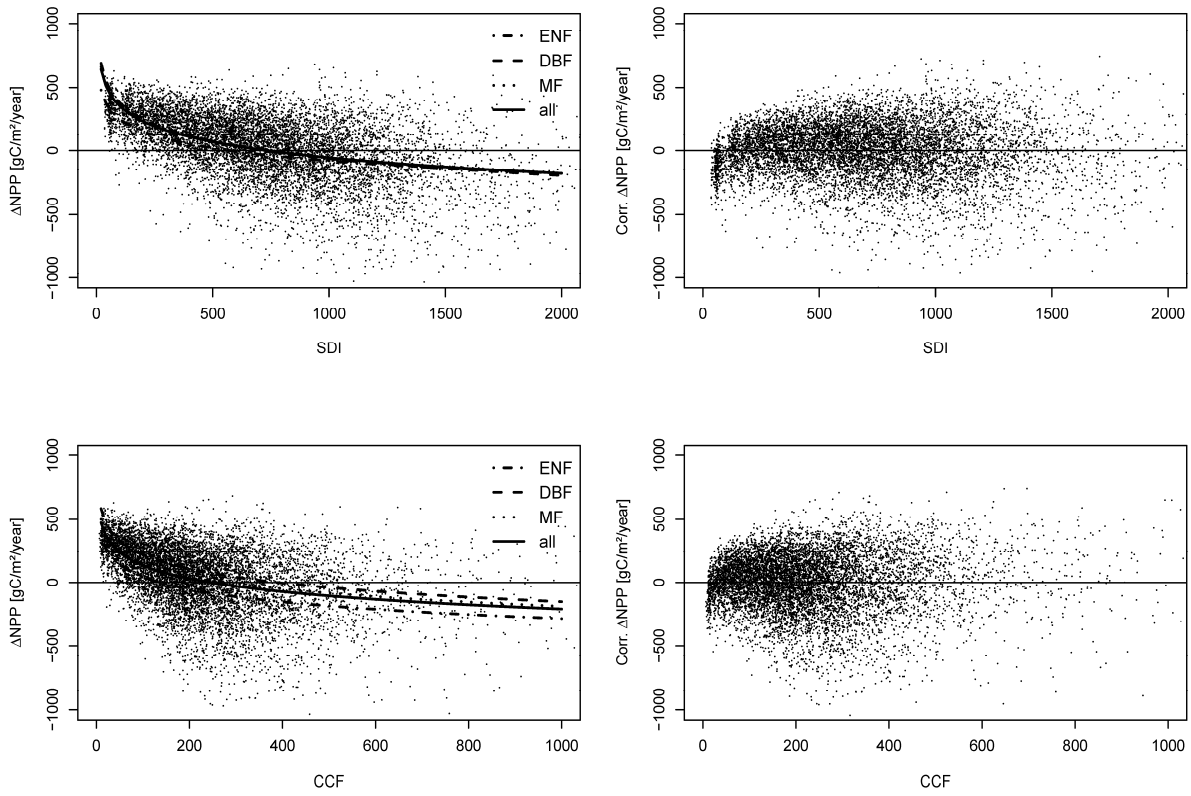

Figure 5. Scatterplots of NPP difference (ΔNPP) and stand density dependent trend curves using SDI (**top left**) and CCF (**bottom left**), the trend curves are calculated for MODIS forest land cover types separately (ENF = evergreen needleleaf forest, DBF = deciduous broadleaf forest, MF = mixed forest) and for all land cover types together (all). The images on the right side (Corr. ΔNPP) show the NPP difference after correcting for stand density given by the trend lines using all plots (all).

Table 2. Coefficients and statistics of trend curves displayed in Figure 5 a,b coefficients for Equations (15) and (16), SE standard error of coefficients, r^2 coefficient of determination, n degrees of freedom.

Depending Variable		a	SE a	b	SE b	r²	n
SDI	ENF	908.3	83.0	−143.0	13.1	0.30	277
	DBF	1265.8	194.7	−192.2	31.6	0.34	71
	MF	1203.3	38.1	−181.3	6.0	0.26	2516
	all	1181.0	19.4	−178.7	3.0	0.28	8716
CCF	ENF	694.8	60.0	−141.3	12.2	0.33	277
	DBF	951.3	145.1	−159.5	26.5	0.34	71
	MF	841.9	30.1	−148.8	30.1	0.21	2516
	all	812.4	15.1	−147.6	2.9	0.22	8716

A variance analysis reveal no significant differences in the parameter estimates *a* and *b* given in Table 2 between the major forest biome types represented by the MODIS land cover types. This suggests that for Austrian forests no biome type specific parameters are needed (Figure 5).

We remove the stand density bias from MODIS NPP using Equation (15), where *a* equals 1181.0 and *b* −178.7, and Equation (16), where *a* equals 812.4 and *b* −147.6 (Table 2). The detrended MODIS NPP features a mean of 515.5 gC/m^2/year, standard deviation 181.7 gC/m^2/year and compared to terrestrial NPP a RMSE of 227.8 gC/m^2/year. After removing the stand density related trend, the difference between the two NPP assessment methods do not exhibit a bias as shown in the right-hand images in Figure 5 (*SDI* $r^2 \leq 0.01$, *CCF* $r^2 \leq 0.01$) than when using the original MODIS NPP results on the left side of Figure 5.

4.4. Consistency of the NPP Estimates across Scales

From the distinct stand density related trend in Figures 4 and 5, we learn that stand density needs to be taken into consideration to provide consistent and comparable results across scales. To ensure that our findings are also consistent across the heterogeneity of the forests across Austria, we test our data for potential variations according to key forest site and stand parameters: (i) ecoregion; (ii) dominant tree species; (iii) mean stand age and (iv) elevation of a given forest inventory plot.

Austria has very distinct biogeographic growth conditions due to the east-west alignment of the Alps. According to Kilian *et al.* [31], these differences lead to nine typical ecoregions (see Figure 1), which are characterized by similar environmental, macro-climatic and geological conditions leading to differences in the potential vegetation.

Ecoregions strongly affect the species distribution. Thus, we next group our data by dominant tree species according to the main relative proportion of the basal area at a given inventory plot (see data section). Norway Spruce and Silver Fir, as more shade-tolerant species, are combined in one group (*PA + AA*). The light demanding tree species Scots Pine and European Larch form the group (*PS + LD*) and the group "*other C*" combines all other coniferous trees. The broadleaf species groups are the Common Beech (*FS*), the Oak (*QS*) and *other B,* which summarizes all other broadleaf species. The left images in Figure 6 show the difference between MODIS and terrestrial NPP estimates grouped by ecoregion. The differences are in general positive, both for ecoregions and tree species, before correcting for stand density. The right images show that correcting for stand density reduces this (Figure 6).

Austrian forests grow across a large gradient in elevation, which affects species and growing conditions. Again, we also group all our data by the following elevation classes: (i) <500 m; (ii) 500–1000 m; (iii) 1000–1500 m; (iv) 1500–2000 m and (v) >2000 m in elevation. The same procedure is applied for the mean stand age at a given inventory plot to assess if any age related influences of our findings exist. The six age classes across all data are: (i) <30 years; (ii) 30–60; (iii) 60–90; (iv) 90–120; (v) 120–150; and (vi) >150 years. The same pattern as in the previous Figure 6 is apparent in Figure 7 as well.

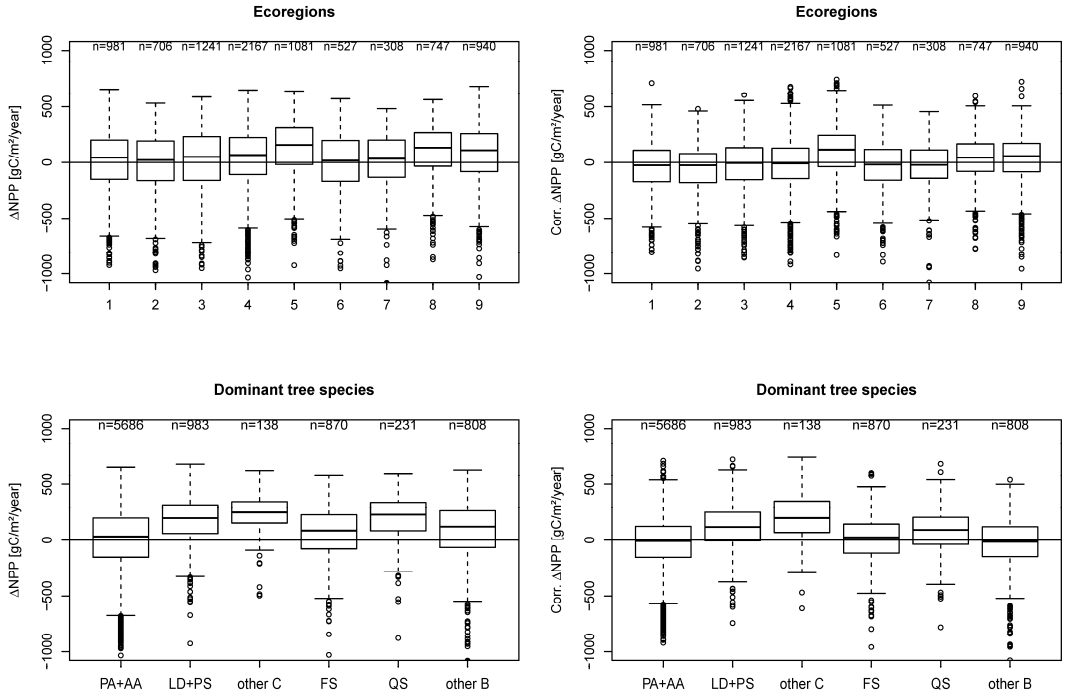

Figure 6. Difference between MODIS NPP and NFI NPP (MODIS minus NFI) grouped by ecoregions (**top**) and dominant tree species (**bottom**). Left original MODIS NPP (ΔNPP) is used, right the detrended MODIS NPP (Corr. ΔNPP) is used. Properties of illustration analogous to Figure 2.

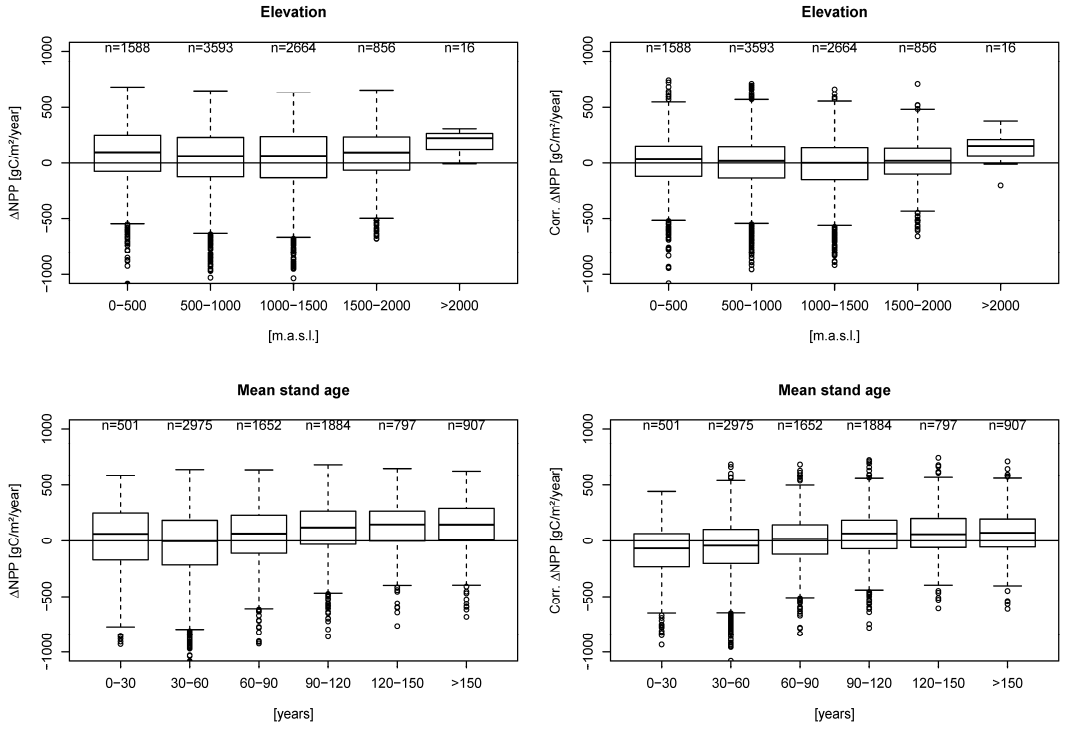

Figure 7. Difference between MODIS NPP and NFI NPP (MODIS minus NFI) grouped by elevation (**top**) and mean stand age (**bottom**). Left original MODIS NPP (ΔNPP) is used, right the detrended MODIS NPP (Corr. ΔNPP) is used. Properties of illustration analogous to Figure 2.

4.5. Effect of Water Availability

Water availability is an important driver of tree productivity. Within the MODIS NPP calculations [50], this is an integral part because daily climate data are required for predicting both GPP and NPP. In a previous study by Pan *et al.* [2], similar discrepancies in comparing the "space-based" MODIS NPP with "ground-based" terrestrial NPP were reported. Pan *et al.* [2] concluded that water availability may be a limiting factor and proposed an "available soil water index" for improving and/or "correcting" MODIS NPP computations compared to terrestrial data. To test this hypothesis and analyze the effect of the water availability on our data, a water balance deficit index is calculated for each inventory plot as an estimate for water limitation according to the following procedure:

$$WBD = ET0 / P \tag{17}$$

$$ET0 = p \times (0.46 \times T + 8) \times 365 \tag{18}$$

WBD is the water balance deficit index which is the ratio of *ET0* potential evapotranspiration and *P* precipitation with *ET0* [mm] of the period 2000–2010 estimated with the method of Blaney-Criddle [51] and *P* the mean annual precipitation 2000–2010 [mm]. *p* is a function of latitude ($p = 0.2729$ for a latitude of 47.5° N) and *T* the mean annual temperature between 2000 and 2010 [°C]. Values of *WBD* less than 1 indicate a lack in available water, while values higher 1 exhibit water availability greater than evapotranspiration. All data are grouped into five *WBD*-classes: (i) <0.5; (ii) 0.5–1.0; (iii) 1.0–1.5; (iv) 1.5 – 2.0 and (v) <2.0.

Figure 8 shows a consisted overestimation of terrestrial NPP by MODIS NPP throughout the different *WBD*-classes when using the original MODIS NPP. The right image in Figure 8 shows that addressing stand density effects reduces this overestimation substantially.

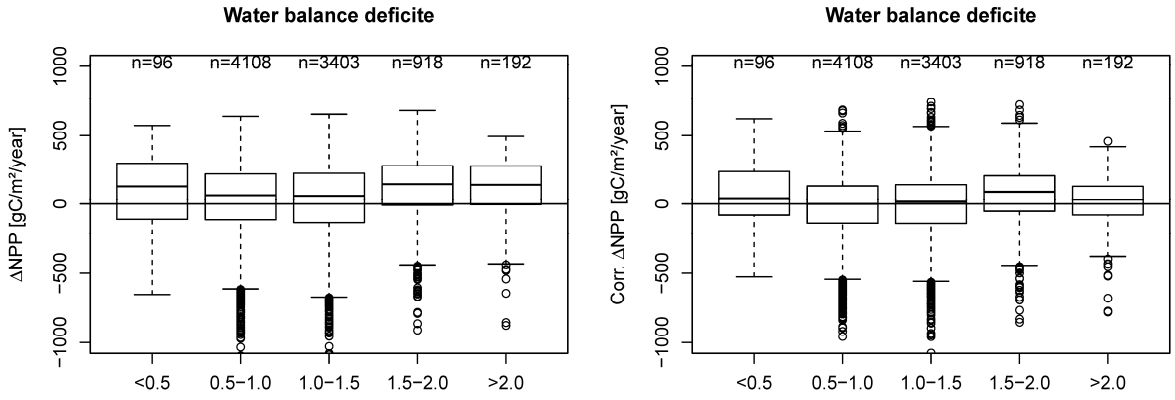

Figure 8. Difference between MODIS NPP and NFI NPP (MODIS minus NFI) grouped by Water balance deficit. Left original MODIS NPP (ΔNPP) is used, right the detrended MODIS NPP (Corr. ΔNPP) is used. Properties of illustration analogous to Figure 2.

5. Discussion

Obtaining daily local climate data (Austrian National Weather Centre ZAMG) for running the MOD17 algorithm reflects the heterogenity of the Austrian landscape more realistically and thus improves the resulting predictions [15]. The ZAMG data set uses more than 200 daily weather stations

across Austria while the NCEP2 (NCEP_DOE_II) [42] and GMAO (NASA Global Modeling and Assimilation Offices) [41] include less than 40 stations. In addition, the spatial resolution of the ZAMG data set is at 0.0083 × 0.0083° (approx. 1 × 1 km). This resolution is more detailed than the two global climate data sets GMAO (0.5 × 0.67°), and NCEP2 (1.875 × 1.875°). This is an additional explanation for the higher accuracy in the local data set. Since the NPP is strongly driven by daily climate data [44] the variation of the resulting predictions using the Austrian local climate data set (ZAMG) is higher but better reflects the existing growing conditions (Figure 2).

The NPP estimates derived from 8939 plots of the National Austrian Forest Inventory (NFI) exhibit an Austrian average of 486.3 gC/m^2/year (standard deviation 244.3 gC/m^2/year). Applying the MODIS NPP algorithm using the local Austrian climate data (ZAMG) result in an average of 579.8 gC/m^2/year (standard deviation 113.4 gC/m^2/year). This is a difference between the means of 93.5 gC/m^2/year.

Such differences may have several reasons. For instance, the BPLUTs might not be appropriate for European forest conditions. The difference could also be explained by inconsistency in the definition of NPP (inventory data represent trees with dbh > 5 cm, MODIS LAI all vegetation on a 1 × 1 km pixel). Other issues could be missing fineroot turnover rates in terrestrial NPP calculations, missing carbon increment of trees that died between the inventory measurements or differences in the spatial resolution of the two products. The terrestrial NPP estimates, *SDI* and *CCF*, are calculated based on the stem numbers in Equations (5)–(7). Thus, any variation in *SDI* or *CCF* directly reflects differences in the coverage of the forest area with trees. In our study of Austrian forests, we assume that the detected differences in MODIS *versus* terrestrial NPP (see Figures 3 and 4) estimates are mainly caused by forest management. However, other events also result in changes to stand density (e.g., wind, drought stress, *etc.*). The observed trend by *SDI* [26] and *CCF* [27] (Figures 3 and 4) and the fact that no other analyzed variable (Figures 6–8) can explain the detected apparent deviations of the two NPP estimates supports the hypothesis of Hasenauer *et al.* [3]. Our results thus coincide with Hasenauer *et al.* [3], that MODIS NPP estimates provide the productivity of fully stocked forests, which are represented only by forest areas without recent changes in stand density.

Forest management, such as thinning operations, instantly reduces volume increment per unit area but concentrates the remaining volume increment to fewer trees [52]. Stand density therefore strongly affects tree diameter development. Terrestrial NPP estimates based on diameter or height data are directly affected by any changes in stand density, while the NPP estimates provided by the MODIS NPP algorithm are not. As long as interventions do not strongly reduce the spectral signal of red and near infrared—the two bands used to derive the MODIS inputs FPAR and LAI—forest management is not well detected by satellite-driven NPP estimates (see Figure 3).

The stand density pattern is also consistent when plotting only the results for each of the major vegetation or biome types represented by the MODIS land cover types (Figure 4). In this study, regression analysis and exponential trend curves are used to quantify the stand density related trend similar to Hasenauer *et al.* [3]. The resulting regression curves fitted using *SDI* and *CCF* in Equations (15) and (16) exhibit a consistent trend, no matter whether fitted by biome type or for all available plots. No clustering effect by biome type is evident, suggesting that one density-driven correction function adjusts for the bias in the NPP predictions across scales (Table 2, Figure 5).

Both competition measures (*SDI* and *CCF*) show a very similar behavior (see Figures 3–5). However, for this dataset, *SDI* gives a slightly higher coefficient of determination (Table 2) and seems

to better address the recorded competition that exists within Austrian National Forest inventory plots. As shown in Figures 6 and 7, ignoring stand density effects will cause overestimation by MODIS NPP estimates by ecoregions and dominant tree species (see Figure 6), elevation and mean stand age (see Figure 7). Applying the correction function leads to a substantial improvement in the consistency of the different NPP results, and consistent and unbiased results across multiple scales can be expected.

The fact that terrestrial NPP overestimates MODIS NPP at high stand densities ($SDI > 1000$ or $CCF > 500$) can be explained with the variable "plot size" of the inventory plots according to the breast height diameter of the trees on a given plot [20]. Thus, the terrestrial NPP estimates based on angle count sample data may have a large random variation and this differs substantially from the terrestrial plot data for deriving NPP as outlined in Hasenauer *et al.* [3] who used fixed area research plots with an area of 2500 m^2.

Pan *et al.* [2] also observed differences between MODIS and terrestrial NPP. They hypothesized that soil water constraints may be a limiting factor and proposed an "available soil water index" for adjusting MODIS NPP computations compared to terrestrial data. Our results of growth conditions in Austrian forests, however, suggest that stand density explains the observed discrepancy as the results grouped by water balance index show a systematic overestimation of terrestrial NPP by MODIS NPP (Figure 8). Correcting for stand density results in a better agreement of MODIS and terrestrial NPP across different "available soil water indices".

One important concern of our study was if large-scale disturbances like bark beetle outbreaks or windthrow [53,54] may have had an impact on our productivity results by method. Disturbances reduce the stand density of forests in a similar manner to management. In our available data from the Austrian Forest inventory, disturbances can be detected with a recorded variable explaining the reason for sample tree death or removal [17]. There are 484 plots (5% of all plots) where, between 2007 and 2009, at least one tree with "random removal" was recorded and, thus, were affected by the disturbances between 2000 and 2002 and between 2007 and 2009. These plots have a median NPP of 464.7 $gC/m^2/year$, which is only slightly lower than the median NPP of all 8939 plots (486.3 $gC/m^2/year$). While disturbances might have big impacts on small scales like forest stands or single inventory plots, they only have a limited and insignificant effect as compared to the forest productivity of Austria.

6. Conclusions

The MODIS NPP model represents all forest vegetation within a 1 × 1 km resolution, assumes fully stocked forest stands and cannot effectively detect management influence in FPAR and LAI. Thus, the effect of forest management, which changes the carbon allocation patterns and, as a consequence, the tree dimensions, is not well represented by MODIS driven NPP estimates. Terrestrial NPP, on the other hand, represents only NPP of trees bigger than the diameter threshold and captures the response of trees to management and, thus, the actual carbon allocation.

Using daily local climate data with high spatial resolution improves the agreement between MODIS NPP and terrestrial NPP.

Correcting the observed stand density related bias in MODIS NPP and thus combining the "space-based" MODIS productivity estimates and "ground-based" national forest inventory data

provide consistent and continuous forest productivity estimates. The corrected MODIS NPP has more agreement with forest inventory data. A better agreement of MODIS and terrestrial NPP estimates allows using MODIS for large-scale forest resource estimates in areas with forest management.

Forest productivity across large scales is of increasing interest as more demands are made on forest resources [55] as well as in the context of REDD (Reducing Emissions from Deforestation and Forest Degradation) [56]. This is of particular importance for areas where no or little terrestrial information on forest productivity is available. With this paper, we provide a conceptual outline of how realistic forest productivity estimates can be derived by combining satellite-driven NPP estimates, such as results from the MODIS NPP algorithm, with stand density estimates (using terrestrial or remote-sensing data) in order to enhance forest productivity predictions across multiple scales.

Acknowledgments

This work is part of the project "*Comparing satellite versus ground driven carbon estimates for Austrian Forests*" (MOTI). We are grateful for the financial support provided by the Energy Fund of the Federal State of Austria—managed by Kommunalkredit Public Consulting GmbH under contract number K10AC1K00050. MT. The NTSG work is funded by NASA Earth Observing System MODIS project (grant NNH09ZDA001N-TERRA-AQUA). We thank the editors and the anonymous reviewers for their helpful comments, which substantially improved the quality of this work. We further want to thank Adam Moreno for proof reading the manuscript.

Author Contributions

Mathias Neumann did the comparative analysis of the results, prepared images and tables and wrote the manuscript. Maosheng Zhao did the calculation of MODIS NPP using different climate data and revised the chapters on the MODIS NPP calculations. Georg Kindermann provided the tree carbon results using the Austrian forest inventory data and revised the chapters on forest inventory data and carbon estimation method. Hubert Hasenauer provided the climate data for Austria and revised the whole manuscript.

Conflicts of Interest

The authors declare no conflict of interest.

Appendix

Carbon estimation and calculation of crown width using NFI data

The carbon increment calculation require carbon estimates for each tree on a given inventory plot. For our study, we use the same method as applied by the Institute of Forest Inventory, Federal Research Centre for Forest, the agency responsible for the National Forest Inventory in Austria. The total dry carbon tree estimate of a single tree, C_i, is calculated as follows:

$$C_i = CC \times (dsm + dbm + dfm + drm) \quad \text{(A1)}$$

where *CC* is the carbon content and considered to be 0.5 for all species [26], *dsm* is the dry stem mass, *dbm* the dry branch mass, *dfm* the dry foliage mass and *drm* the dry root mass.

Dry stem biomass (*dsm*) is calculated using stem volume and species-specific conversion factors. Stem volume (V_{tree}) is derived from the tree measurements diameter at breast height (*dbh*), total tree height *(h*) and the species-specific form factor (*FF*). The calculated volume represents the stem excluding aboveground part of the stump and the branches [17,57,58].

$$dsm = V_{tree} \times wd \times \frac{100 - sf}{100} \tag{A2}$$

$$V_{tree} = \left(\frac{dbh}{200}\right)^2 \times \pi \times h \times FF \tag{A3}$$

where V_{tree} is the stem volume of a single tree [m³], *wd* is the dry wood density [t BM/m³], *sf* the shrinkage factor by tree species [%], *dbh* the diameter at breast height (1.3 m), *h* the tree height, *d*03 the diameter at 30% of tree height and *hc* the crown height (height to the crown base). The form factor (*FF*) reduces the volume of the cylinder to the actual tree form. The Austrian Forest Inventory uses two different form factor functions: one for the trees with *dbh* ranging from 5–10.4 cm with the following form,

$$FF = c_1 + c_2 \times \ln^2(dbh) + c_3 / h + c_4 / dbh + c_5 / dbh + c_6 \quad dbh \quad h + c_7 \quad dbh \quad h \tag{A4}$$

and a second one for all trees with a *dbh*≥10.4 cm:

$$FF = c_0 + c_1 \times d03 / dbh + c_2 \times (d03 / h)^2 + c_3 \times h / dbh + c_4 \times h / dbh + c_5 / dbh + c_6 \times hc / h \tag{A5}$$

c_i are species-specific parameter estimates for calculating stem volume used by the Austrian Forest Inventory given in Tables A1 and A2 [17,57,59]. The conversion factors *wd* and *sf* according to Wagenführ and Scheiber [60] are given in Table A3. Note that for Equation (A3) *dbh* [cm] and *h* [m], while in Equations (A4,A5) the *d*03, *dbh*, *hc* and *h* [dm].

Table A1. Coefficients used in models for volume for trees with dbh 5.0–10.4 cm (Schieler [59] cited in Gabler and Schadauer [17]).

Species Name	c1	c2	c3	c4	c5	c6	c7
Picea abies, other coniferous	0.5634	−0.1273	−8.5502	0	0	7.6331	0
Abies alba	0.5607	0.1547	−0.6558	0.0332	0	0	0
Larix decidua	0.4873	0	−2.0429	0	0	5.9995	0
Pinus sylvestris, Pinus strobus	0.4359	−0.0149	5.2109	0	0.0287	0	0
Pinus nigra	0.5344	−0.0076	0	0	0	0	2.2414
Pinus cembra	0.5257	−0.0335	7.3894	−0.1065	0	0	3.3448
Fagus sylvatica, other broadleaf	0.5173	0	−13.6214	0	0	9.9888	0
Quercus sp.	0.4171	0.2194	13.3259	0	0	0	0
Carpinus betulus	0.3247	0.0243	0	0.2397	0	−9.9388	0
Fraxinus sp., Sorbus sp., Prunus sp.	0.4812	−0.0149	−10.831	0	0	9.3936	0
Acer sp.	0.5010	−0.0352	−8.0718	0	0.0352	0	0
Ulmus sp.	0.4422	−0.0245	0	0	0	0	2.8771
Betula sp.	0.4283	−0.0664	0	0	0	8.4307	0
Alnus sp.	0.3874	0	7.1712	0.0441	0	0	0

Table A1. *Cont.*

Species Name	c1	c2	c3	c4	c5	c6	c7
Populus sp.	0.3664	0	1.1332	0.1306	0	0	0
Salix sp.	0.5401	−0.0272	−25.1145	0.0833	0	9.3988	0

Table A2. Coefficients used in models for volume for trees with dbh≥10.4 cm (Braun [57] cited in Gabler and Schadauer [17]).

Species Name	c0	c1	c2	c3	c4	c5	c6
Picea abies, other coniferous	−0.2436	0.8271	0	2.91E-04	0	0.0287	0
Abies alba	0.0991	0	0.5126	4.46E-04	0	0.0160	0
Larix decidua	−0.2198	0.8028	0	3.24E-04	0	0.0184	0
Pinus sylvestris	−0.2099	0.8140	0	1.96E-04	0	0.0317	0
Pinus nigra, Pinus strobus	−0.1929	0.8479	0	2.04E-04	0	0.0069	0
Pinus cembra	0.0501	0.4676	0	1.57E-04	0	0.0761	0
Fagus sylvatica, other	−0.1309	0.6743	0	0	1.67E-04	0	0.0668
Quercus sp.	0.1852	0	0.3501	0	4.77E-04	0	0.0657
Carpinus betulus	0.0421	0.4226	0	0	4.21E-04	0	0.0770
Fraxinus sp.	−0.0198	0.5124	0	0	4.70E-04	0	0.0535
Acer sp.	−0.0286	0.5655	0	0	2.37E-04	0	0.0083
Ulmus sp.	−0.1390	0.6950	0	0	3.18E-04	0	0.0166
Betula sp.	−0.0778	0.5682	0	0	5.54E-04	0	0.0517
Alnus sp.	−0.1646	0.7038	0	0	2.59E-04	0	0.0589
Populus tremula	−0.1456	0.6657	0	0	4.18E-04	0	0.0589
Populus alba	−0.1438	0.6487	0	0	5.62E-04	0	0.0812
Populus nigra	−0.0843	0.5928	0	0	6.47E-04	0	0.0227
Salix sp.	−0.1376	0.6944	0	0	4.59E-04	0	0.0128

Table A3. Conversion factors for stem biomass [60].

Species Name	wd	sf
Picea sp.	0.41	11.80
Abies sp.	0.41	11.85
Larix sp.	0.55	13.20
Pinus sylvestris, other Pinus	0.51	11.80
Pinus nigra	0.56	11.80
Pinus cembra	0.40	9.00
Pinus strobus	0.37	9.00
Pseudotsuga menziesii	0.47	12.00
Taxus baccata	0.64	8.80
Fagus sylvatica, other hardwood broadleaf	0.68	17.50
Carpinus betulus	0.67	13.60
Quercus sp.	0.75	18.80
Fraxinus sp.	0.67	13.20
Acer sp.	0.59	11.65
Ulmus sp.	0.64	12.80
Castanea sativa	0.56	11.45
Robinia pseudacacia	0.73	11.80

Table A3. *Cont.*

Species Name	wd	sf
Prunus sp., Sorbus sp.	0.57	13.85
Sorbus domestica	0.71	17.15
Sorbus aucuparia	0.62	18.60
Betula sp.	0.64	13.95
Alnus sp.	0.49	13.40
Tilia sp., other softwood broadleaf	0.52	14.65
Populus sp.	0.45	11.90
Populus nigra	0.41	12.50
Salix sp.	0.52	9.60
Juglans regia	0.64	13.70
Juglans nigra	0.56	12.65
Ostrya carpinifolia	0.75	18.80
Malus, Pyrus	0.70	14.40

For the remaining biomass components (*dbm, dfm*, *drm*), we use allometric biomass functions developed for Austrian forest conditions, which are also used by the Austrian National Forest Inventory.

The dry branch biomass *dbm* [kg] for *Pinus sp.* is calculated with a *dbh* [cm] and *h* [m] dependent equation [61],

$$dbm = 1.0366 \cdot e^{(-2.8762+2.04516\cdot\ln(dbh)-0.07025\cdot\ln(h))} \quad \text{(A6)}$$

We use equations from Ledermann and Neumann [62] for all other tree species. If height to the life crown measurements (*hc)* are available, models using *dbh*, *h* and *hc* as input variables are used according to Equation (A8). If *hc* is missing, models with *dbh* and *h* are used according to Equation (A7) [62]:

$$dbm = l2 \cdot e^{b_{20}+b_{21}\cdot\ln(dbh)+b_{22}\cdot\frac{h}{dbh})} \quad \text{(A7)}$$

$$dbm = l3 \cdot e^{b_{30}+b_{31}\cdot\ln(dbh)+b_{32}\cdot\frac{h}{dbh}+b_{33}\cdot\ln(CR)} \quad \text{(A8)}$$

$$CR = \frac{h-hc}{h} \quad \text{(A9)}$$

where *CR* is the crown ratio and all other variables as previously defined. The species-specific parameters b_i, *l2* and *l3* are given in Table A4**.**

Table A4. Coefficients used in models for biomass in branches [62].

Species Name	b20	b21	b22	l2	b30	b31	b32	b33	l3
Picea abies, other	-	1.7459	-	1.102	-	2.0252	0.1451	0.9154	1.051
Abies alba	-	2.0429	-	1.105	-	2.2066	0	0.4384	1.087
Fagus sylvatica, other BL	-	2.3930	-	1.251	-	2.5568	-	0.6002	1.212
Quercus sp.	1.8554	0.9332	-	1.334	-	1.9445	0	1.2137	1.280
Carpinus betulus	-	2.8913	-	1.181	-	2.8281	0	0.9318	1.130

For coniferous trees, the foliage biomass (*dfm*) is included in the branch biomass calculations (*dbm*) as outlined above. For the deciduous trees, *dfm* [kg] is calculated using allometric functions according to *dbh*. These functions are based on measurements collected by Burger [63,64] and are modified after Lexer and Hönninger [65].

$$dfm = a_0 \times dbh^{a_1} \tag{A10}$$

The species-specific parameters a_i are given in Table A5.

The root biomass (*drm*) in [kg] is defined as roots with a minimum diameter of 2 mm including the root stump. For *Pinus sylvestris* and *Pinus nigra* the allometric function of Offenthaler and Hochbichler [66] is used:

$$drm = 0.038872 \times dbh^{2.066783} \tag{A11}$$

For all other species, the following dbh and age-dependent model is applied [67,68]:

$$drm = c_0 \cdot e^{c_1 + c_2 \cdot \ln(dbh) + c_3 \cdot \ln^2(dbh) + c_4 \cdot \ln(age)} \tag{A12}$$

dbh in [cm], *age* is the tree age [a], c_i are species-specific parameter according to [67,68].

The species-specific parameters c_i are given along with the parameters for foliage biomass in the Table A5.

Table A5. Coefficients c_i used in models for biomass in roots ([67] for "Coniferous (except Pinus sp.)", [68] for "Fagus sylvatica, other broadleaf", [66] for "Quercus sp." and "Carpinus betulus") and *a0* and *a1* for biomass in foliage [63–65].

Name	c0	c1	c2	c3	c4	a0	a1
Coniferous (except Pinus sp.)	1.041	−8.350	4.568	−0.330	0.281	-	-
Fagus sylvatica, other broadleaf	1.080	−4.000	2.320	0	0	0.022	2.300
Quercus sp.	1.051	−3.975	2.523	0	0	0.135	1.811
Carpinus betulus	1.052	−3.848	2.488	0	0	0.022	2.300

Equation (A13) estimates maximum crown width of a tree assuming open-grown conditions for calculating *CCF* [27]. The species-specific parameters to calculate maximum crown width are given in Table A6.

$$CW_i = e^{c_0 + c_1 \cdot \ln(dbh)} \tag{A13}$$

Table A6. Coefficients used for maximum crown width [29].

Name	c0	c1
Picea abies, other coniferous	−0.3232	0.6441
Abies alba	0.0920	0.5380
Larix decidua	−0.3396	0.6823
Pinus sylvestris, other Pinus sp.	−0.1797	0.6267
Pinus nigra	−0.1570	0.6310
Pinus cembra	−1.3154	0.8288
Fagus sylvatica, other broadleaf	0.2662	0.6072
Quercus sp., Castanea sativa	−0.3973	0.7328
Acer sp., Betula sp., Alnus sp., Populus sp., Salix sp., Ulmus sp.	0.4180	0.5285

Table A6. *Cont.*

Name	c0	c1
Fraxinus sp., Robinia, sp. Prunus sp. Sorbus sp.	0.1366	0.6183
Tilia sp.	0.1783	0.5665

References

1. Shvidenko, A.; Schepaschenko, D.; McCallum, I.; Santoro, M.; Schmullius, C. Use of remote sensing products in a terrestrial ecosystems verified full carbon account: Experiences from Russia. In Proceedings of the International Institute for Applied Systems Analysis: Earth Observation for Land-Atmosphere Interaction Science, Frascati, Italy, 3–5 November 2010.
2. Pan, Y.; Birdsey, R.; Hom, J.; McCullough K.; Clark, K. Improved estimates of net primary productivity from MODIS satellite data at regional and local scales. *Ecol. Appl.* **2006**, *16*, 125–132.
3. Hasenauer, H.; Petritsch, R.; Zhao, M.; Boisvenus, C.; Running, S.W. Reconciling satellite with ground data to estimate forest productivity at national scales. *For. Ecol. Manag.* **2012**, *276*, 196–208.
4. Tomppo, E.; Gschwantner, T.; Lawrence, M.; McRoberts, R.E. *National Forest Inventories: Pathways for Common Reporting*; Springer: Berlin, Germany, 2010; p. 610.
5. Schadauer, K.; Gschwantner, T.; Gabler, K. Austrian National Forest Inventory: Caught in the Past and Heading toward the Future. In Proceedings of the Seventh Annual Forest Inventory and Analysis Symposium, Washington, DC, USA, 3–6 October 2005; pp. 47–53.
6. Hasenauer, H.; Eastaugh, C.S. Assessing forest production using terrestrial monitoring data. *Int. J. For. Res.* **2012**, doi:10.1155/2012/961576.
7. Running, S.; Nemani, R.; Heinsch, F.; Zhao, M.; Reeves, M.; Hashimoto, H. A continuous satellite-derived measure of global terrestrial primary production. *BioScience* **2004**, *54*, 547–560.
8. Zhao M.; Running S.W. Drought-induced reduction in global terrestrial net primary production from 2000 through 2009. *Science* **2010**, *329*, 940–943.
9. Monteith, J. Solar radiation and productivity in tropical ecosystems. *J. Appl. Ecol.* **1972**, *9*, 747–766.
10. Thornton, P.E.; Running, S.; White, M. Generating surfaces of daily meteorological variables over large regions of complex terrain. *J. Hydrol.* **1997**, *190*, 214–251.
11. Van Tuyl, S.; Law, B.E.; Turner, D.P.; Gitelman, A.I. Variability in net primary production and carbon storage in biomass across Oregon forests—An assessment integrating data from forest inventories, intensive sites, and remote sensing. *For. Ecol. Manag.* **2005**, *209*, 273–291.
12. Waring, R.H.; Milner, K.S.; Jolly, W.M.; Phillips, L.; McWethy, D. Assessment of site index and forest growth capacity across the Pacific and Inland Northwest USA with MODIS satellite-derived vegetation index. *For. Ecol. Manag.* **2006**, *228*, 285–291.
13. Muukkonen, P.; Heiskanen, J. Biomass estimation over a large area based on standwise forest inventory data and ASTER and MODIS satellite data: A possibility to verify carbon inventories. *Remote Sens. Environ.* **2007**, *107*, 617–624.

14. Härkönen, S.; Lehtonen, A.; Eerikäinen, K.; Mäkelä, A. Estimating forest carbon fluxes for large regions based on process-based modelling, NFI data and Landsat satellite images. *For. Ecol. Manag.* **2011**, *262*, 2364–2377.
15. Eenmäe, A.; Nilson, T.; Lang, M. A note on meteorological variables related trends in the MODIS NPP product for Estonia. *For. Stud./Metsanduslikud. Uurim.* **2011**, *55*, 60–63.
16. Fang, H.; Wei, S.; Liang, S. Validation of MODIS and CYCLOPES LAI products using global field measurement data. *Remote Sens. Environ.* **2012**, *119*, 43–54.
17. Gabler, K.; Schadauer, K. Methods of the Austrian forest inventory 2000/02 origins, approaches, design, sampling, data models, evaluation and calculation of standard error. Available online: http://bfw.ac.at/rz/bfwcms.web?dok=7518 (accessed on 30 March 2015).
18. He, L.; Chen, J.M.; Pan, Y.; Birdsey, R.; Kattge, J. Relationships between net primary productivity and forest stand age in U.S. forests. *Glob. Biogeochem. Cycles* **2012**, *26*, 1–19.
19. Liu, C.; Westman, C.; Berg, B.; Kutsch, W.; Wang, G.Z.; Man, R.; Ilvesniemi, H. Variation in litterfall-climate relationships between coniferous and broadleaf forests in Eurasia. *Glob. Ecol. Biogeogr.* **2004**, *13*, 105–115.
20. Bitterlich, W. Die Winkelzaehlprobe. *Allg. For. Holzwirtsch. Ztg.* **1948**, *59*, 4–5.
21. Englisch, M.; Karrer, G.; Mutsch, F. Österreichische Waldboden-Zustandsinventur. Teil 1: Methodische Grundlagen. *Mitt. Forstichen Bundesver. Wien.* **1992**, *168*, 5–22.
22. Schieler, K. Methode der Zuwachsberechnung der Oesterreichischen Waldinventur. Ph.D. Thesis, University of Natural Resources and Applied Life Sciences, Institute of Forest Growth, Vienna, Austria, 1997; p. 92.
23. Van Deusen, P.C.; Dell, T.R.; Thomas, C.E. Volume Growth Estimation from Permanent Horizontal Points. *For. Sci.* **1986**, *32*, 415–422.
24. Eastaugh, C.S.; Hasenauer, H. Biases in Volume Increment Estimates Derived from Successive Angle Count Sampling. *For. Sci.* **2013**, *59*, 1–14.
25. Martin, G.L. A method for estimating ingrowth on permanent horizontal sample points. *For. Sci.* **1982**, *28*, 110–114.
26. *Intergovernmental Panel on Climate Change, Good Practice Guidance for Land Use, Land-Use Change and Forestry*; Institute for Global Environmental Strategies (IGES): Hayama, Japan, 2003; p. 590.
27. Krajicek, J.E.; Brinkman, K.A.; Gingrich, S.F. Crown competition—A measure of density. *For. Sci.* **1961**, *1*, 35–42.
28. Reinecke, L.H. Prefecting a stand density index for even-aged forest. *J. Agric. Res.* **1933**, *46*, 627–638.
29. Hasenauer, H. Dimensional relationships of open-grown trees in Austria. *For. Ecol. Manag.* **1997**, *96*, 197–206.
30. Hasenauer, H.; Burkhart, H.; Sterba, H. Variation in potential volume yield of loblolly pine plantations. *For. Sci.* **1994**, *40*, 162–176.
31. Kilian, W.; Müller, F.; Starlinger, F. Die forstlichen Wuchsgebiete Österreichs—Eine Naturraumgliederung nach waldökologischen Gesichtspunkten. Available online: http://bfw.ac.at/030/2377.html (accessed on 27 March 2015).

32. Hasenauer, H.; Merganičová, K.; Petritsch, R.; Pietsch, S.A.; Thornton, P.E. Validating daily climate interpolations over complex terrain in Austria. *Agric. For. Meteorol.* **2003**, *119*, 87–107.
33. Eastaugh, C.S.; Petritsch, R.; Hasenauer, H. Climate characteristics across the Austrian forest estate from 1960 to 2008. *Aust. J. For. Sci.* **2010**, *127*, 133–146.
34. Thornton, P.E.; Hasenauer, H.; White, M.A. Simultaneous estimation of daily solar radiation and humidity from observed temperature and precipitation: An application over complex terrain in Austria. *Agric. For. Meteorol.* **2000**, *104*, 255–271.
35. Petritsch, R.; Hasenauer H. Climate input parameters for real-time online risk assessment. *Nat. Hazards* **2011**, *59*, 1–14.
36. Zhao, M.; Heinsch, F.A.; Nemani, R.R.; Running, S.W. Improvements of the MODIS terrestrial gross and net primary production global data set. *Remote Sens. Environ.* **2005**, *95*, 164–175.
37. Wang, Y.; Woodcock, C.E.; Buermann, W.; Stenberg, P.; Voipio, P.; Smolander, H.; Hame, T.; Tian, Y.; Hu, J.; Knyazikhin, Y.; Myneni, R.B. Evaluation of the MODIS LAI algorithm at a coniferous forest site in Finland. *Remote Sens. Environ.* **2004**, *91*, 114–127.
38. Tan, B.; Woodcock, C.; Hu, J.; Zhang, P.; Ozdogan, M.; Huang, D.; Yang, W.; Knyazikhin, Y.; Myneni, R. The impact of gridding artifacts on the local spatial properties of MODIS data: Implications for validation, compositing, and band–to–band registration across resolutions. *Remote Sens. Environ.* **2006**, *105*, 98–114.
39. Yang, W.; Tan, B.; Huang, D.; Rautiainen, M.; Shabanov, N.V.; Wang, Y.; Privette, J.L.; Hummerich, K.F.; Fensholt, R.; Sandolt, I.; *et al.* MODIS leaf area index products: From validation to algorithm improvement. *IEEE Trans. Geosci. Remote Sens.* **2006**, *44*, 1885–1898.
40. Friedl, M.; Sulla-Menashe, D.; Tan, B.; Schneider, A.; Ramankutty, N.; Sibley, A.; Huang, X. MODIS Collection 5 global land cover: Algorithm refinements and characterization of new datasets. *Remote Sens. Environ.* **2010**, *114*, 168–182.
41. Ma, L.; Zhang, T.; Li, Q.; Frauenfeld, O.W.; Qin, D. Evaluation of ERA-40, NCEP-1, and NCEP-2 reanalysis air temperatures with ground-based measurements in China. *J. Geophys. Res.* **2008**, *113*, 1–15.
42. Kanamitsu, M.; Ebisuzaki, W.; Woollen, J.; Yang, S.K.; Hnilo, J.J.; Fiorino, M.; Potter, G.L. NCEP-DOE AMIP-II reanalysis (R-2). *Bull. Am. Meteorol. Soc.* **2002**, *83*, 1631–1643.
43. Weng, Q. *Global Urban Monitoring and Assessment through Earth Observation*; CRC Press: Boca Raton, FL, USA, 2014; p. 440.
44. Zhao, M.; Running, S.W.; Nemani, R.R. Sensitivity of moderate resolution imaging spectroradiometer (MODIS) terrestrial primary production to the accuracy of meteorological reanalyses. *J. Geophys. Res.* **2006**, *111*, 1–13.
45. Bruce, D. Yield Differences between Research Plots and Managed Forests. *J. For.* **1977**, *75*, 14–17.
46. Hradetzky, J. Concerning the precision of growth estimation using permanent horizontal point samples. *For. Ecol. Manag.* **1995**, *71*, 203–210.
47. Austrian Forest Act (Österreichisches Forstgesetz). Available online: https://www.ris.bka.gv.at/ (accessed on 4 February 2015).
48. Eastaugh, C.; Hasenauer, H. Improved estimates of per-plot basal area from angle count inventories. *Forests* **2014**, *7*, 178–185.

49. Seidl, R.; Eastaugh, C.S.; Kramer, K.; Maroschek, M.; Reyer, C.; Socha, J.; Vacchiano, G.; Zlatanov, T.; Hasenauer, H. Scaling issues in forest ecosystem management and how to address them with models. *Eur. J. For. Res.* **2013**, *132*, 653–666.
50. Zhang, K.; Kimball, J.S.; Mu, Q.; Jones, L.A.; Goetz, S.J.; Running, S.W. Satellite based analysis of northern ET trends and associated changes in the regional water balance from 1983 to 2005. *J. Hydrol.* **2009**, *379*, 92–110.
51. Blaney, H.F.; Criddle, W.D. *Determining Water Requirements in Irrigated Areas from Climatological and Irrigation Data*; Technical Paper; United States Department of Agriculture: Washington, WA, USA, 1950 ; Volume 96, p. 44.
52. Assmann, E. *The Principles of Forest Yield Study*; Pergamon Press: New York, NY, USA, 1970; p. 506.
53. Seidl, R.; Rammer, R.; Jäger, D.; Lexer, M.J. Impact of bark beetle (*Ips. typographus* L.) disturbance on timber production and carbon sequestration in different management strategies under climate change. *For. Ecol. Manag.* **2008**, *256*, 209–220.
54. Seidl, R.; Fernandes, P.M.; Fonseca, T.F.; Gillet, F.; Jönsson, A.M.; Merganicova, K.; Netherer, S.; Arpaci, A.; Bontemps, J.D.; Bugmann, H.; *et al.* Modelling natural disturbances in forest ecosystems: A review. *Ecol. Model.* **2010**, *222*, 903–924.
55. Pan, Y.; Birdsey, R.A.; Fang, J.; Houghton, R.; Kauppi, P.E.; Kurz, W.A.; Phillips, O.L.; Lewis, S.L.; Canadell, J.G.; Ciais, P.; *et al.* A large and persistent carbon sink in the world's forests. *Science* **2011**, *333*, 988–992.
56. Angelsen, A. *Realising REDD+ National Strategy and Policy Options*; CIFOR: Bogor, Indonesia, 2009; p. 390.
57. Braun, R. Österreichische Forstinventur. Methodik der Auswertung und Standardfehler-Berechnung. *Mitt. Forstl. Bundesver. Wien.* **1969**, *84*, 1–60.
58. Pollanschütz, J. Formzahlfunktionen der Hauptbaumarten Österreichs. *Inf. Forstl. Bundesver. Wien.* **1974**, *153*, 341–343.
59. Schieler, K. Methodische Fragen in Zusammenhang mit der österreichischen Forstinventur. Master Thesis, University of Natural Resources and Applied Life Sciences, Institute of Forest Growth, Vienna, Austria, 1988; p. 99.
60. Wagenführ, R.; Scheiber, C. *Holzatlas*, 2nd Ed.; VEB Fachbuchverlag: Leibzig, Germany, 1985; p. 690.
61. Hochbichler, E.; Bellos, P.; Lick, E. Biomass functions for estimating needle and branch biomass of spruce (*Picea abies*) and Scots pine (*Pinus sylvestris*) and branch biomass of beech (*Fagus sylvatica*) and oak (*Quercus robur* and *petrea*). *Aust. J. For. Sci.* **2006**, *123*, 35–46.
62. Ledermann, T.; Neumann, M. Biomass equations from data of old long-term experimental plots. *Aust. J. For. Sci.* **2006**, *123*, 47–64.
63. Burger, H. Holz, Blattmenge und Zuwachs. VIII. Mitteilung. Die Eiche. *Mitt. Schweiz. Anst. Forstl. Vers.* **1947**, *25*, 211–279.
64. Burger, H. Holz, Blattmenge und Zuwachs. X. Mitteilung. Die Buche. *Mitt. Schweiz. Anst. Forstl. Vers.* **1949**, *26*, 419–468.
65. Lexer, M.J.; Hoenninger, K. A modified 3D-patch model for spatially explicit simulation of vegetation composition in heterogeneous landscapes. *For. Ecol. Manag.* **2001**, *144*, 43–65.

66. Offenthaler, I.; Hochbichler, E. Estimation of root biomass of Austrian forest tree species. *Aust. J. For. Sci.* **2006**, *123*, 65–86.
67. Wirth, C.; Schumacher J.; Schulze E.D. Generic biomass functions for Norway spruce in Central Europe—A meta-analysis approach toward prediction and uncertainty estimation. *Tree Physiol.* **2004**, *24*, 121–139.
68. Bolte, A.; Rahmann, T.; Kuhr, M.; Pogoda, P.; Murach, D.; von Gadow, K. Relationships between tree dimension and coarse root biomass in mixed stands of European beech (*Fagus sylvatica* L.) and Norway spruce (*Picea abies*[L.] Karst.). *Plant Soil* **2004**, *264*, 1–11.

© 2015 by the authors; licensee MDPI, Basel, Switzerland. This article is an open access article distributed under the terms and conditions of the Creative Commons Attribution license (http://creativecommons.org/licenses/by/4.0/).